GNSS Augmentation by Low-Earth-Orbit (LEO) Satellites: Integrity Performance Under Non-Ideal Conditions

Sukrut Oak, Sam Pullen, Sherman Lo, Isaiah Colobong, Juan Blanch, and Todd Walter
Stanford University
Mark Crews and Robert Jackson
Lockheed Martin

Abstract

In previous work (Pullen, 2022; Pullen, 2023), we introduced the concept of augmenting GPS with six inclined geosynchronous satellites (I-GEOs) that would provide GPS-Block-III-quality military and civil ranging signals along with conveying Satellite-based Augmentation System (SBAS) messages to users. This would create a new means to distribute SBAS messages globally and would support Advanced Receiver Autonomous Integrity Monitoring (ARAIM) for users not equipped to use SBAS. This paper extends this concept to ranging augmentation from satellites in Low Earth Orbit (LEO) such as those in the current Globalstar, IridiumNext, and OneWeb orbits. For each arrangement of combined GPS and LEO satellites, the Stanford MAAST GNSS simulation software package is used to evaluate the protection levels (error bounds) that would apply to military or civil aviation IFR approaches (such as LPV approaches) for ARAIM users without differential corrections. The first set of "baseline" results are the most optimistic because they assume that ranging signals from LEO satellites have the same error bounds and fault probabilities as do GPS satellites. Since this is unlikely to be the case, sensitivity studies have been performed using MAAST in which the LEO elevation mask angle and per-satellite fault probability are increased above those for GPS. These studies show that the benefits of LEO satellite augmentation of

1. INTRODUCTION

Integrity (safety protection via error bounding and rapid fault alerts) for GNSS applications to aviation, land, and marine vehicles is provided today by Satellite-based and Ground-based Augmentation Systems (SBAS and GBAS, respectively) and various forms of Receiver Autonomous Integrity Monitoring (RAIM). While today's SBAS and GBAS provide only single-frequency (L1 C./A code) corrections, dual-frequency and multi-constellation SBAS and GBAS that also provide corrections on L5/E5a are expected to become available in the nest 10 to 15 years. Users not supported by existing SBAS or GBAS, such as military users of L1/L2 P/Y and M codes, can take advantage of Advanced Receiver Autonomous Integrity Monitoring (ARAIM), which extends the capabilities of earlier forms of RAIM to multiple-failure scenarios and employs more-optimal error bounds.

As explained previously in (Pullen, 2022; Pullen, 2023), the version of ARAIM being developed for civil aviation users ((Blanch, 2015), (Milestone 3, 2016) requires the use of signals from multiple GNSS constellations (e.g., at least GPS and Galileo) to provide high availability for demanding horizontal (e.g., RNP 0.1) and vertical (e.g., LPV) phases of flight. However, in the foreseeable future, U.S. military users will likely be restricted from using GNSS signals not provided or authorized by the U.S. government. This limitation has been explored in our previous work on ARAIM, where the use of Galileo in a limited "constellation check" form was evaluated (Katz, 2021). We have also evaluated improvements to ARAIM performance using improved ARAIM Integrity Support Message (ISM) parameters based upon more intensive GNSS ground monitoring and faster ISM message updates (Pullen, 2021).

In Pullen (2022) and Pullen (2023), we considered the benefits of augmenting GNSS with various constellations of Inclined Geosynchronous (I-GEO) satellites, which would provide GPS-quality L1, L2, and L5 ranging measurements while also providing L1, L2 and L5 SBAS corrections. Dual-frequency SBAS users of these satellites along with GPS were shown to robustly obtain near-100% availability of LPV approach operations (down to 250 ft above the runway threshold), meaning that both the Vertical

Protection Level (VPL) and the 2-D Horizontal Protection Level (HPL) are below the Vertical Alert Limit of 50 meters and the Horizontal Alert Limit of 40 meters (these alert limits specify the boundaries of safe navigation sensor errors).

Because SBAS performance and availability for LPV are so high, our focus has turned to the use of ARAIM by users either unable to use SBAS corrections or who need ARAIM to mitigate significant local errors such as anomalous multipath. Section 2 of this paper summarizes the ARAIM analysis approach and input parameters used in this and earlier simulations, while Section 3 describes the three LEO constellations for which results are provided in this paper. Section 4 describes the baseline results, in which LEO satellite ranging signals are presumed (unrealistically) to be equivalent to GPS, while Section 5 shows results in which two of the GPS inputs (elevation mask angle and per-satellite fault probability) are relaxed (made worse) for LEO signals. Section 6 shows additional results where the VPL and HPL contours (bounding values) are set to the 99.9th percentile instead of the 95th percentile. Section 7 summarizes this paper.

2. ARAIM SIMULATION PROCEDURE AND ISM PARAMETERS

The ARAIM version of Matlab Algorithm Availability Simulation Tool (MAAST) developed by Stanford is used to determine VPL, HPL, and the resulting LPV availability of each user location in the same manner as in our previous work (Pullen, 2021; Pullen, 2022; Pullen, 2023). Briefly, MAAST simulates the satellite geometries observed by a grid of user locations around the world based on Yuma-almanac-formatted definitions of GNSS, GEO, and LEO satellite constellations. At each time epoch, range error biases and standard deviations are computed for each satellite visible at each user location. The baseline ARAIM algorithm ((Blanch, 2015), (Milestone 3, 2016)) is then used to generate a variety of performance indicators for each user location at that time. These indicators (including VPL and HPL) are stored for each user location and time epoch so that post-processing after the satellite geometry simulation completes can determine the VPL and HPL limits for each location along with the availability of LPV approaches (the number of epochs in which both VPL $\leq$ VAL and HPL $\leq$ HAL divided by the total number of epochs). The results presented below are do not focus on the LPV operation but instead show contours of VPL and HPL at the 95th and 99.9th percentiles.

Figure 1 from Pullen (2022) shows the signal-in-space (SIS) components of the error and prior-probability-of-(integrity)-failure models used for GPS (MEO) satellites and I-GEO and LEO satellite augmentations in these simulations. The numbers for GPS satellites are those promised by the U.S. operators of GPS to the International Civil Aviation Organization in support of ARAIM (ICAO, 2020). The improved numbers highlighted in green on the right are those used in these simulations and represent additional ground monitoring of the GPS and augmentation satellites with ISM updates at least daily if needed (Katz, 2021). These values provide the potential for reasonably high availability of vertical ARAIM (meaning in support of applications with demanding requirements on vertical position, such as LPV) even without GEO or LEO augmentations, as will be shown in Section 4.1. The benefit of adding I-GEO or LEO ranging satellites is to increase the visible satellite redundancy such that LPV availability varies less by location and gets closer to the ideal values shown for dual-frequency SBAS in Pullen (2022).

Parameter	GPS Commitment	GPS and LEO SVs (with additional ground monitoring)
URA	in Nav Data (ICD table)	URA = 1.0 m; URE = 0.63 m; bias = 0.35 m
URA Threshold	4.42 × URA	URA Threshold based on P_{sat}
R_{sat}	10^{-5} / hour	$R_{sat} = 5 \times 10^{-7}$ / hour
P_{sat}	10^{-5}	$P_{sat} = 5 \times 10^{-7}$
P_{const}	10^{-8}	$P_{const} = 2.5 \times 10^{-9}$
MFD	1 hour	MFD = 1 hour
TTA	10 seconds	TTA = 10 seconds

Figure 1: *SIS Error and Fault-Model Parameters Used in MAAST ARAIM Simulations (Pullen, 2022)*

3. LOW EARTH ORBIT SATELLITE CONSTELLATIONS

For our study, we tested three different operational LEO satellite constellations to simulate how satellites in the orbits of these constellations would improve ARAIM performance. For all the satellite orbit data, we exported the two-line elements of the available satellites in the constellation from CelesTrak in late 2022 and converted them into the Yuma almanac form that the MAAST ARAIM simulation reads. A summary of the parameters for these constellations is shown in Table 1. Note that, while a few satellites in the CelesTrak orbit data are indicated to be unhealthy, all these LEO satellites are treated as healthy in our ARAIM simulations.

The first constellation we tested was Globalstar, which we chose because of their recent partnership with Apple and possible plans for constellation expansion. For this constellation, there were 85 satellite orbits that we exported for analysis, all of which had an altitude of 1460 km at the equator and an inclination of 52 degrees. The second constellation we chose was IridiumNext, which had a similar number of satellites to Globalstar, with 75 satellite orbits compared to 85 satellite orbits from Globalstar. The IridiumNext satellites had roughly half the altitude of the Globalstar satellites, with an altitude of 775 km at the equator, as well as a much higher inclination of 86.4 degrees, indicating these satellites had near polar orbits. Finally, we chose OneWeb as the third constellation for analysis, which had 583 satellites, almost an order of magnitude greater than the other two constellations. OneWeb satellites had an altitude ranging from 450 to 1210 km at the equator and inclinations ranging from 86.5 degrees to 87.9 degrees. Like IridiumNext's satellite inclinations, OneWeb satellites also had near polar orbits.

Table 1: *Orbital Parameters of Simulated LEO Constellations*

Constellation	Number of Satellites	Semi-major axis *a* (km)	Altitude at Equator (km)	Inclination *i* (deg)
Globalstar	85	7840	1460	52.0
IridiumNext	75	7155	775	91.2
OneWeb	583	6830 – 7590	450 – 1210	86.5 – 87.9

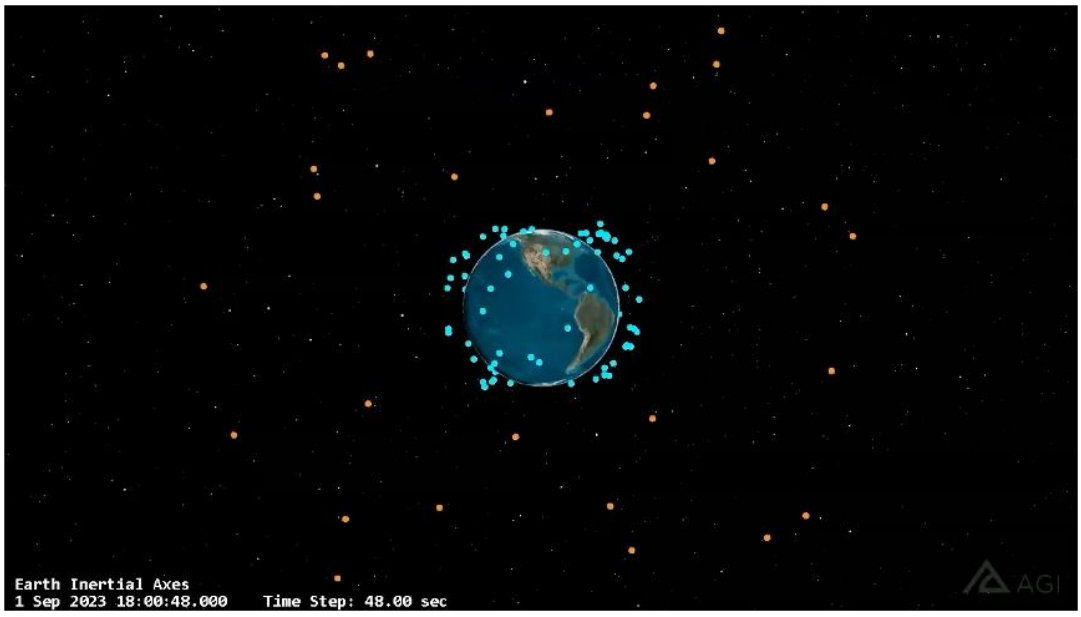

Figure 2: *Visualization of Globalstar Satellite Constellation (Blue) with 30-SV GPS Constellation (Orange)*

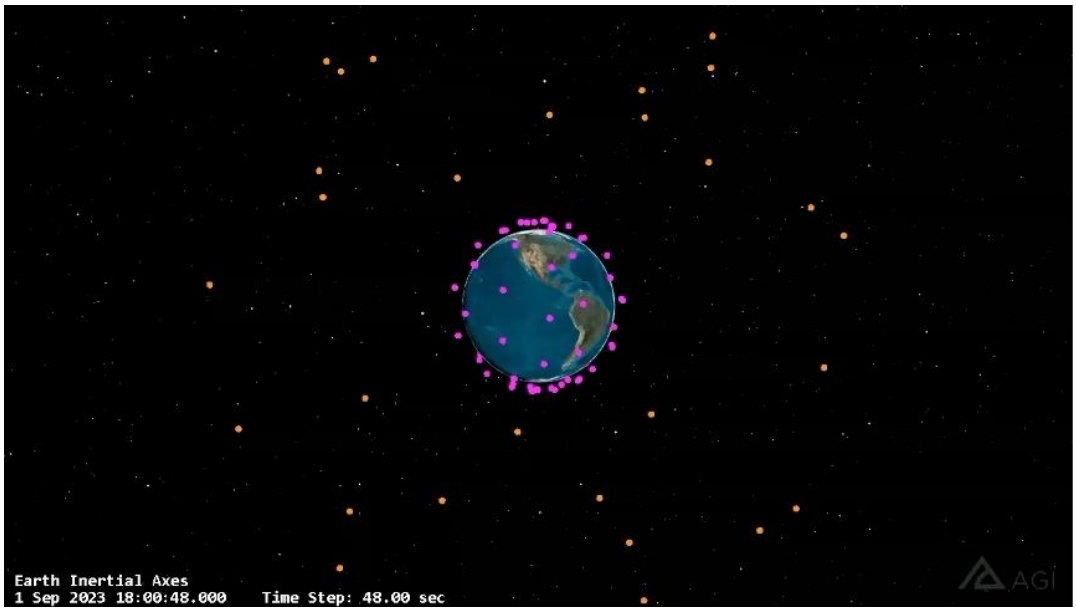

Figure 3: *Visualization of IridiumNext Satellite Constellation (Magenta) with 30-SV GPS Constellation (Orange)*

Figures 2 and 3 show visualizations of the Globalstar and IridiumNext satellite locations along with GPS satellites at a single moment in time (videos of satellite motion over time are available in the presentation slides). Because the Globalstar satellites have a lower inclination compared to the IridiumNext satellites, more Globalstar satellites can be seen from the equatorial and mid latitude regions compared to the number of IridiumNext satellites visible from these areas. Additionally, because IridiumNext's satellite inclinations are near polar, with many of their orbit planes intersecting at the poles, more IridiumNext satellites can be seen from the poles, compared to the number of Globalstar satellites. While the OneWeb satellite constellation is not visualized here, these satellites have similar inclinations to the IridiumNext satellites, making their constellation design closer to the IridiumNext design than the Globalstar design. However, OneWeb's satellites have various altitudes and a much greater number of satellites in their constellation.

4. RESULTS FOR GPS AUGMENTED WITH LEO CONSTELLATIONS (BASELINE)

4.1 GPS Satellites Only

ARAIM results for LPV availability for GPS without I-GEO or LEO satellite augmentation were provided in Pullen (2023) for the baseline 24-Slot GPS constellation defined in Table 3.2-1 of the *GPS SPS Performance Standard* (SPS, 2020). These results are extended to the expandable 24-Slot constellation, which contains 27 or 30 satellites depending on the number of expandable orbit slots used (see Table 3.2-2 of SPS, 2020). In each of the modified orbit planes, the "nearby" satellites are within 10 to 20 degrees on either side of the removed satellite. This provides additional geometric redundancy but does not always improve on the original 4-satellite-per-plane configuration of the 24-Slot constellation.

Figure 4 shows the HPL contour plot on the left and VPL contour plot on the right for the 30-Slot GPS constellation without augmentation (using ARAIM). Note that these contours (and most of the contours that follow) are at the 95th percentile ("95%"), meaning that the colors shown on each map indicate PL values that are exceeded only 5% of the time at the location underneath. Without augmentation, most of the world achieves 95% PLs lower than 50 meters (vertical) and 40 meters (horizontal), HPL performs better, as expected, bounding most of the equatorial and polar regions at less than 25 meters.

The results in Figure 4 are quite good for GPS unaugmented by other GNSS constellations, GEOs, or LEOs. However, they fall well short of the desired 99.9% level of LPV availability, which would require VPLs below 50 meters. In addition, they depend on the additional offline ground monitoring that supports the ISM values shown in Figure 1. Therefore, geometry augmentation by satellites

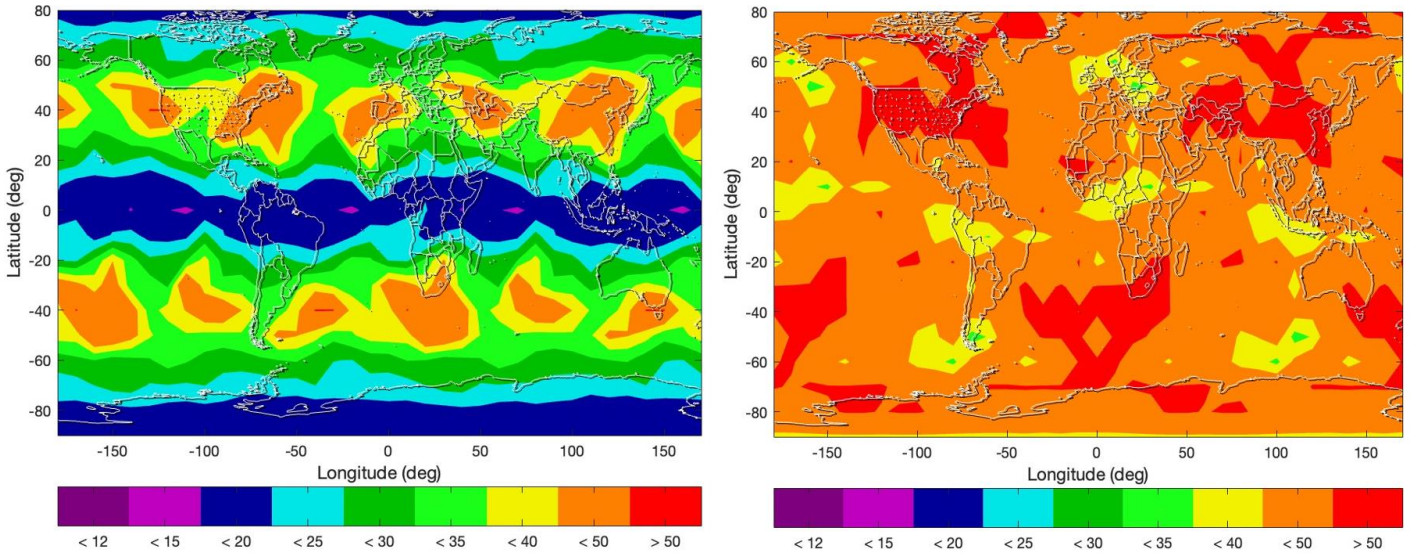

Figure 4: *ARAIM 95th Percentile HPL and VPL Contours for Unaugmented 30-SV GPS Constellation*

that can be used by military and other non-SBAS users would be very helpful, in addition to the benefits of I-GEOs in providing SBAS corrections.

4.2 GPS with Baseline LEO Augmentation

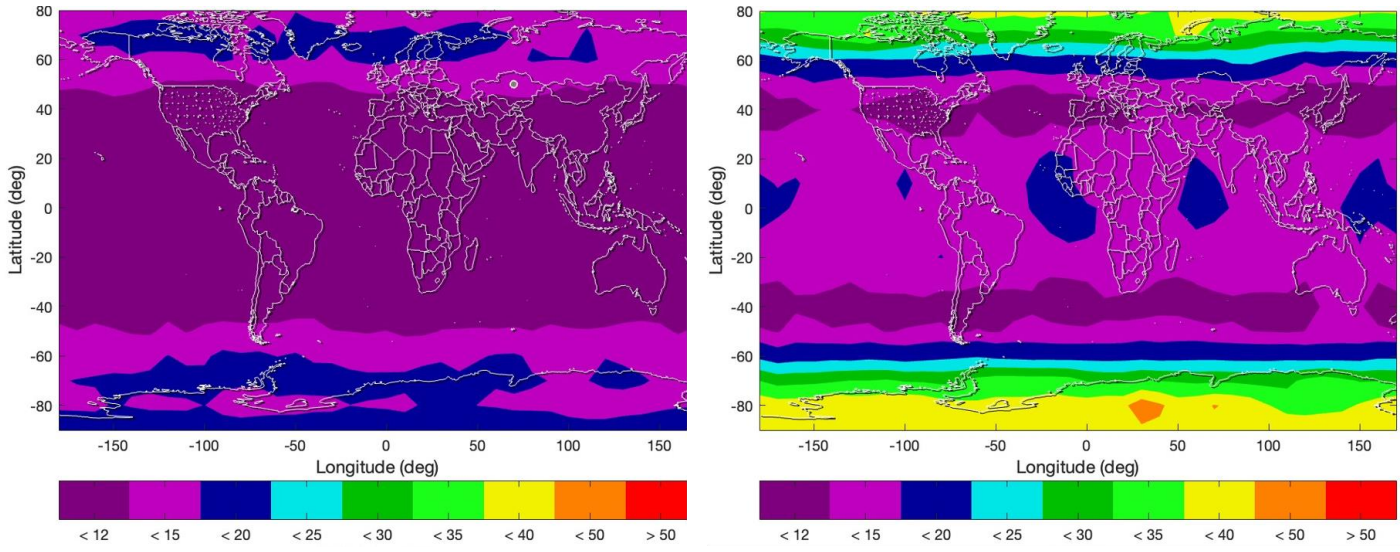

Figure 5: *ARAIM 95th Percentile HPL and VPL for 30-SV GPS and Baseline Globalstar Constellation*

Figure 5 shows the 95% ARAIM HPL and VPL contour plots for the 30-SV GPS constellation augmented by the baseline Globalstar constellation of 85 satellites downloaded from CelesTrak. Adding these satellites greatly improves both the HPL and VPL contours compared to the GPS-only constellation results. Because Globalstar satellites have an inclination of about 52 degrees, the best performance can be seen by ARAIM users near the equatorial regions and mid-latitudes. As users move farther away from the equator, performance decreases, with the worst bounds found at the poles. For both HPL and VPL, the integrity bounds are almost all less than 15 meters, providing significant improvement compared to HPL and VPL for GPS only.

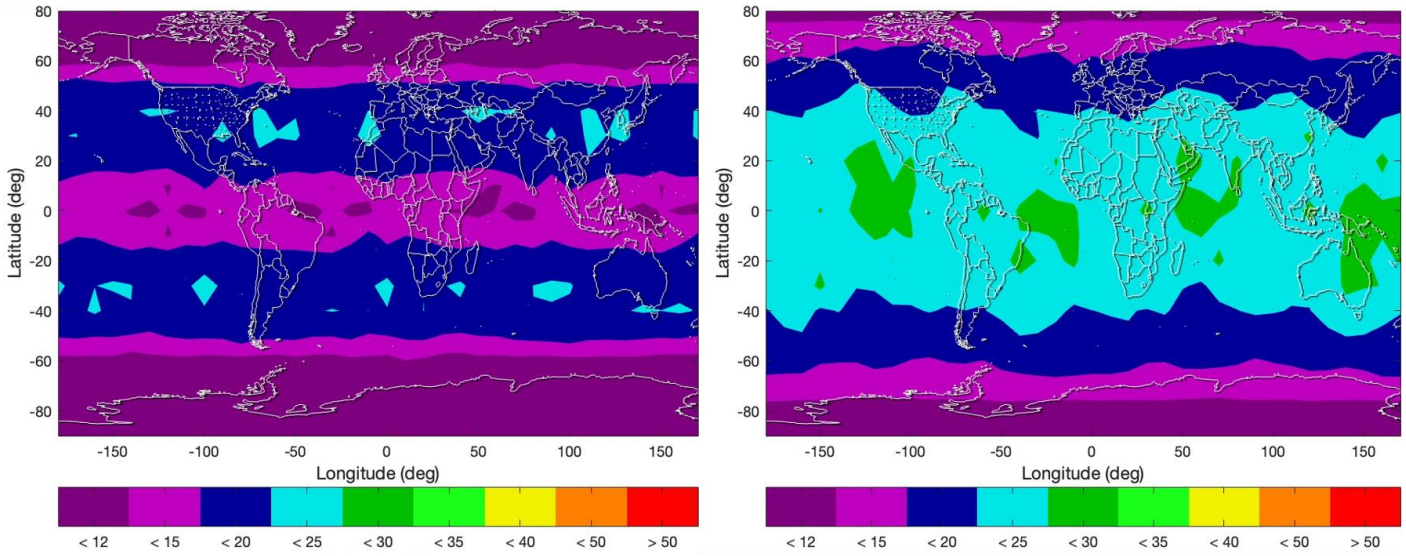

Figure 6: *ARAIM 95th Percentile HPL and VPL for 30-SV GPS and Baseline IridiumNext Constellations*

Figure 6 shows the 95% HPL and VPL contour plots for the 30-SV GPS constellation augmented by 75 IridiumNext satellites from the downloaded CelesTrak orbit elements. Compared to the Globalstar satellite augmentation, IridiumNext performance is slightly weaker overall for both HPL and VPL. However, compared to the GPS-only baseline results, there are still great improvements, with global HPL mostly less than 20 meters and global VPL mostly less than 25 meters. Note that these contours form a different pattern than the ones generated by Globalstar augmentation, largely due to differences in their satellite inclination angles. While Globalstar satellites have lower inclinations, IridiumNext satellites have much higher inclinations that are near polar, which means that their orbit planes intersect near the poles, and more satellites will be visible from these regions. Thus, the best performance for the augmentation is for ARAIM users near the poles, with both 95% HPLs and VPLs limited to less than 12 meters. As the analysis gets closer to the equatorial and mid latitude regions, performance degrades gradually, with a drop of 1 to 3 contour levels (color bands) from less than 12 meters to less than 20 or 25 meters.

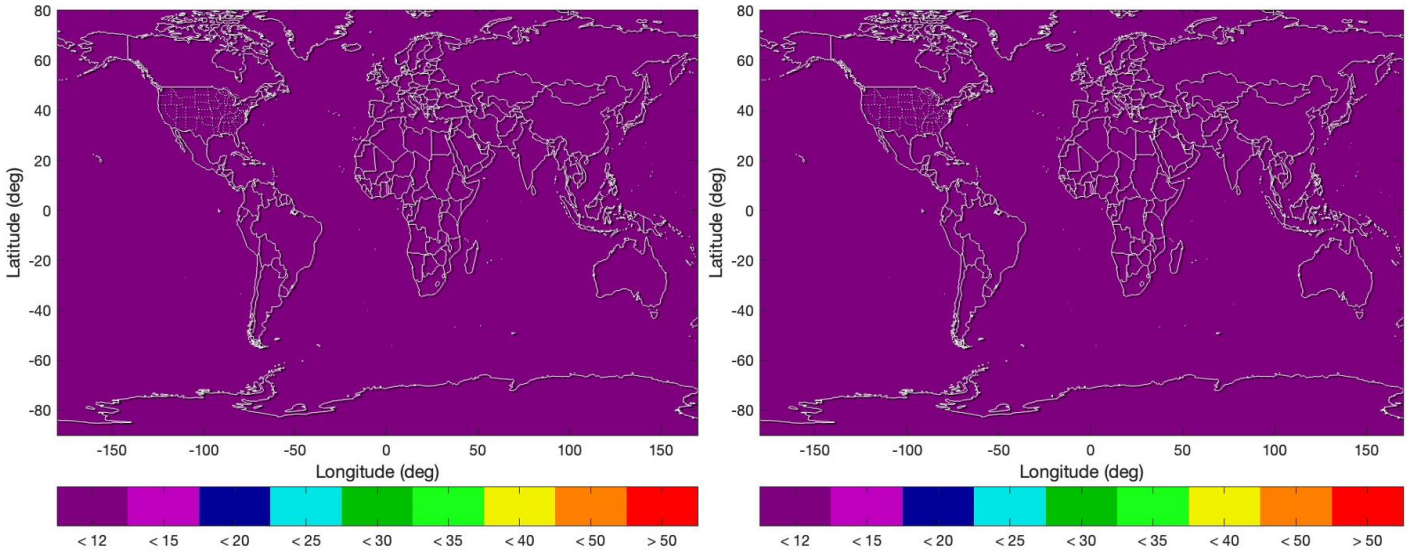

Figure 7: *ARAIM 95th Percentile HPL and VPL for 30-SV GPS and Baseline OneWeb Constellations*

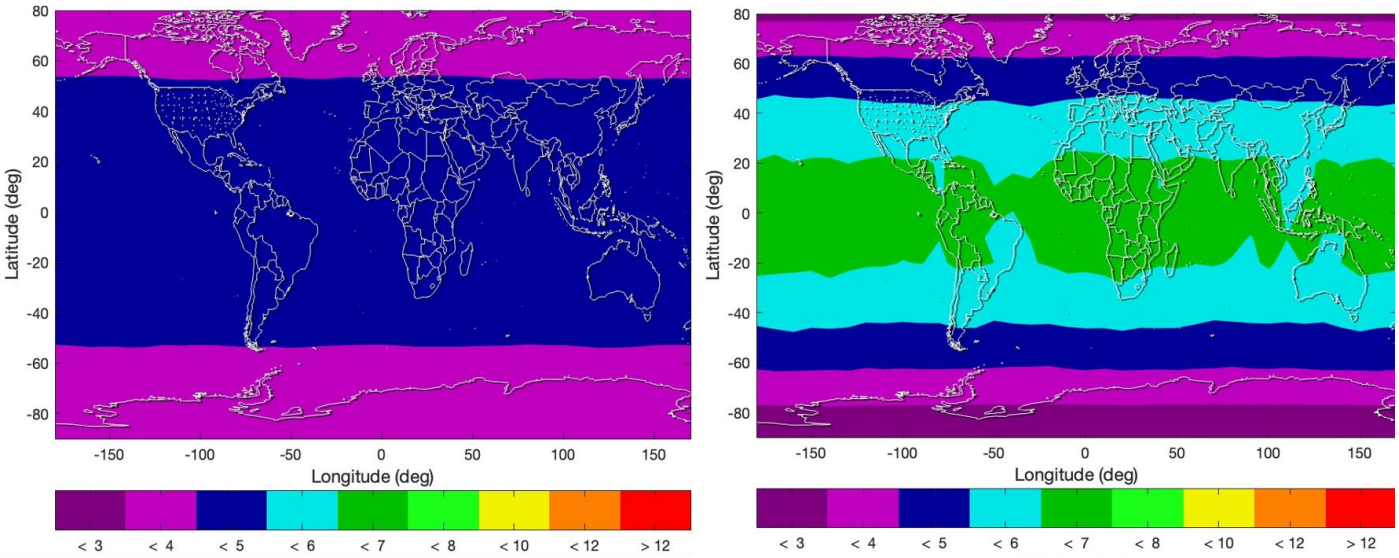

Figure 8: *ARAIM 95th Percentile HPL and VPL for 30-SV GPS and Baseline OneWeb Constellations (Zoomed In)*

Figure 7 shows the 95% HPL and VPL contour plots for the 30-SV GPS constellation augmented by 583 OneWeb satellites from the CelesTrak orbit elements. With almost 600 OneWeb satellites, augmentation by this constellation provides wonderful results, with global 95% HPL and VPL levels less than 12 meters for all users. Although these results are very idealistic and are generated with the optimistic assumptions shown in Figure 1, it is interesting to understand how low these levels can become. Therefore, the same chart was regenerated with a zoomed in scale, which can be found in the zoomed-in contour scale of Figure 8. The level to which the protection levels decrease becomes staggering. The 95% HPLs are globally below 5 meters, and the 95% VPLs are globally below 7 meters. Compared to the GPS Baseline results and the other constellation augmentations, OneWeb with the baseline assumptions for LEO satellite behavior provides dramatic improvements in global protection levels, both horizontally and vertically. Of course, these results were generated using very generous assumptions for the LEO augmentation satellite parameters. However, these baseline results provide a "best case scenario" from which more realistic assumptions can be applied.

5. RESULTS FOR LEO-AUGMENTED GPS WITH LESS-OPTIMISTIC PARAMETERS

5.1 GPS with LEO Augmentation with Less-Optimistic Mask Angles

Now that the baseline results with ideal LEO parameters have been described, more realistic assumptions can be applied to the LEO satellite constellations. These changes were applied in the ARAIM code base to produce the following results, with the GPS parameters and assumptions remaining untouched. First, variations in the mask angle were explored to understand how and to what degree the protection levels are worsened by increases in the mask angle. Next, variations in the p_{sat}, or probability of a one satellite out fault, were explored to understand the effects on the protection levels. Finally, several combinations of more realistic assumptions for both the mask angle and p_{sat} were generated, initiating the process of adjusting the parameters to use more realistic assumptions.

The contour plots in Figures 9 are the same Globalstar results presented in Figure 5. The contour plots in Figures 10 and 11 are generated using the same parameters as from Figure 9 except for the elevation mask angle (minimum satellite elevation for user visibility), which is increased from the baseline of 5° for LEO satellites. Figure 10 displays how the protection levels deteriorate when changing the mask angle to 15°, and Figure 11 displays how the protection levels deteriorate even further when changing the mask angle to 30°. From 5° to 15° degrees and again from 15° to 30°, the contours generally change by one or two color bands, representing degradations of about 5 to 10 meters in the protection levels. Overall, the Globalstar result pattern remains constant, with the best performance for the ARAIM users near the equator and mid latitudes and degraded performance approaching the poles.

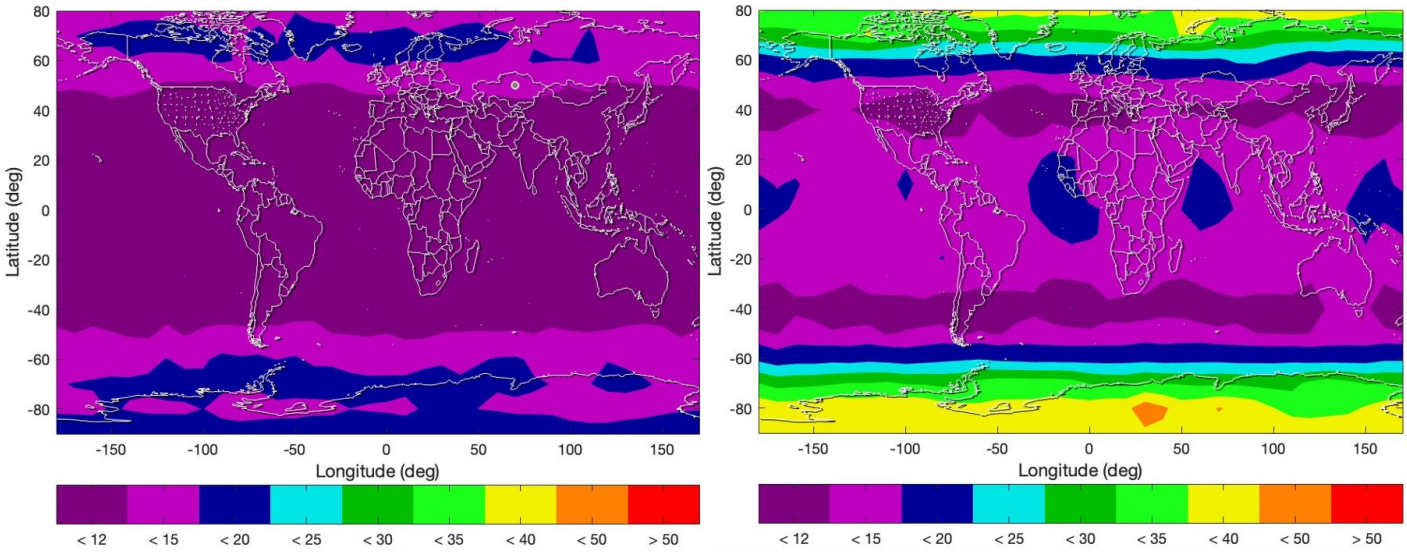

Figure 9: *ARAIM 95th Percentile HPL and VPL for 30-SV GPS and Globalstar Satellites with 5° Mask Angle*

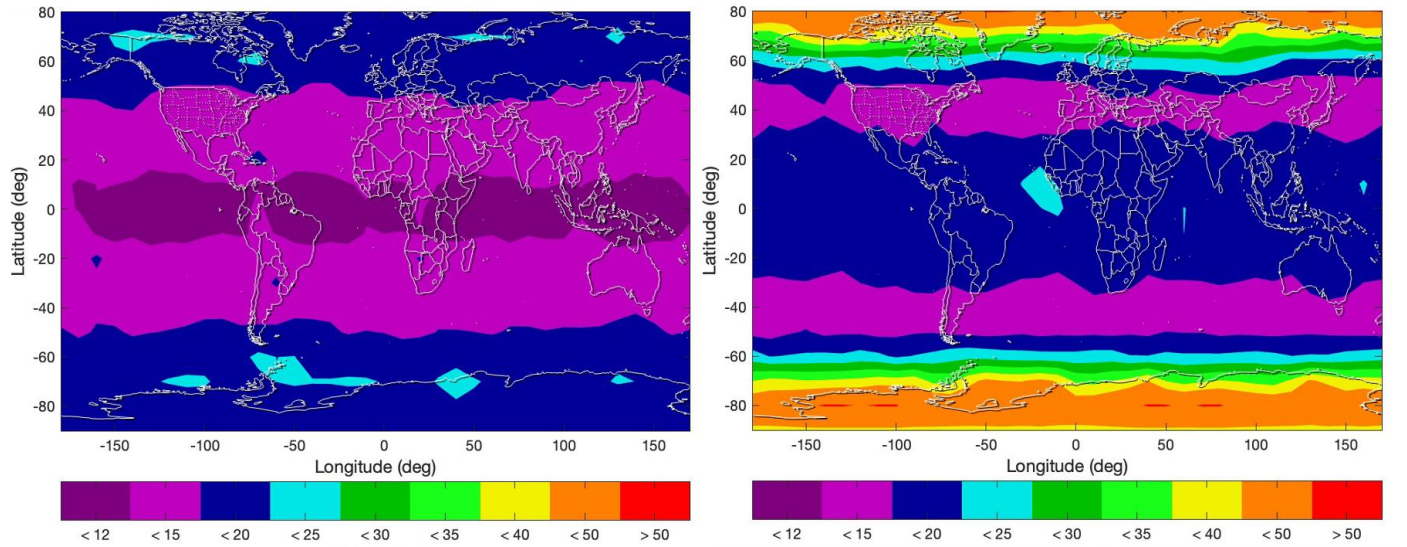

Figure 10: *ARAIM 95th Percentile HPL and VPL for 30-SV GPS and Globalstar Satellites with 15° Mask Angle*

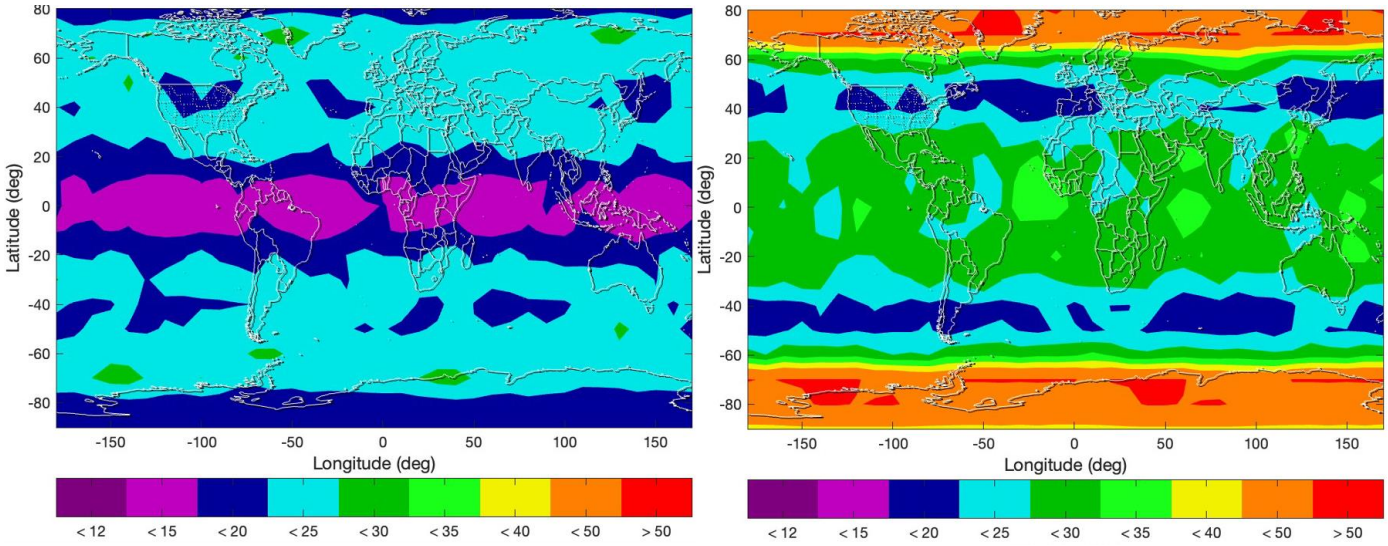

Figure 11: *ARAIM 95th Percentile HPL and VPL for 30-SV GPS and Globalstar Satellites with 30° Mask Angle*

As with the previous three Globalstar figures, Figures 12 through 14 show the protection-level contour plots of the GPS constellation augmented by IridiumNext with various mask angles. The contour plots in Figures 12 are the same IridiumNext results presented in Figure 6, and the contour plots in Figures 13 and 14 are generated using mask angles increased from the baseline of 5°. Figure 13 displays how the protection levels deteriorate when changing the mask angle to 15°, and Figure 14 displays how the protection levels deteriorate further when changing the mask angle to 30°. In the same manner as the Globalstar results angle, the contours generally change by one or two colors when the mask angle is increased by one increment, representing degradations of about 5 to 10 meters in the protection levels. Similarly, the pattern also remains constant, with the best performance for users near the poles and degraded performance in the equatorial and mid-latitude regions. Interestingly, at the edge of the polar regions, there are areas where increasing the mask angle from 5° to 30° has little or no effect on the protection levels. This is likely due to the large number of IridiumNext satellites visible at the poles, since the orbit planes for the entire constellation intersect in these areas.

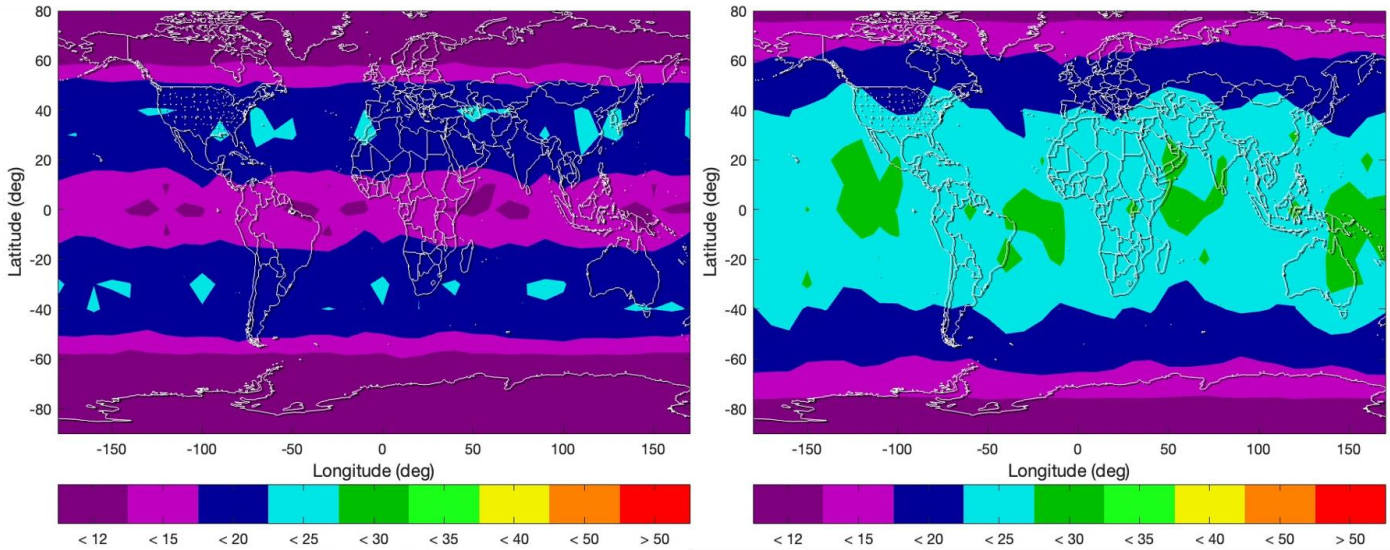

Figure 12: *ARAIM 95th Percentile HPL and VPL for 30-SV GPS and IridiumNext Satellites with 5° Mask Angle*

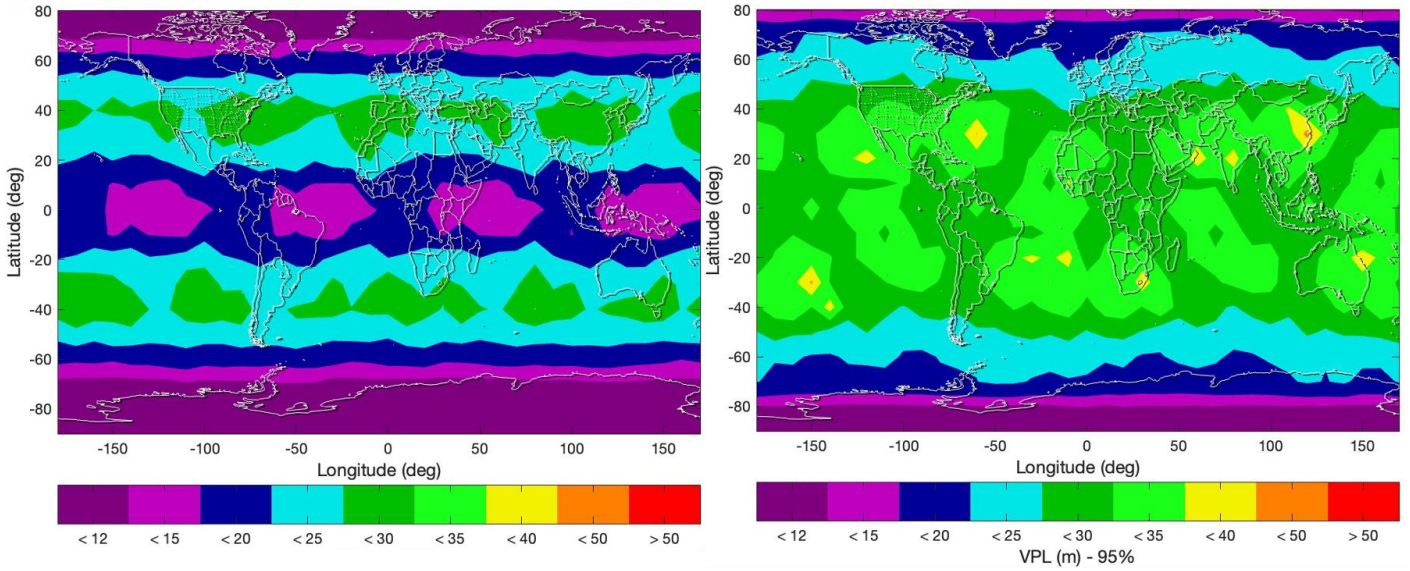

Figure 13: *ARAIM 95th Percentile HPL and VPL for 30-SV GPS and IridiumNext Satellites with 15° Mask Angle*

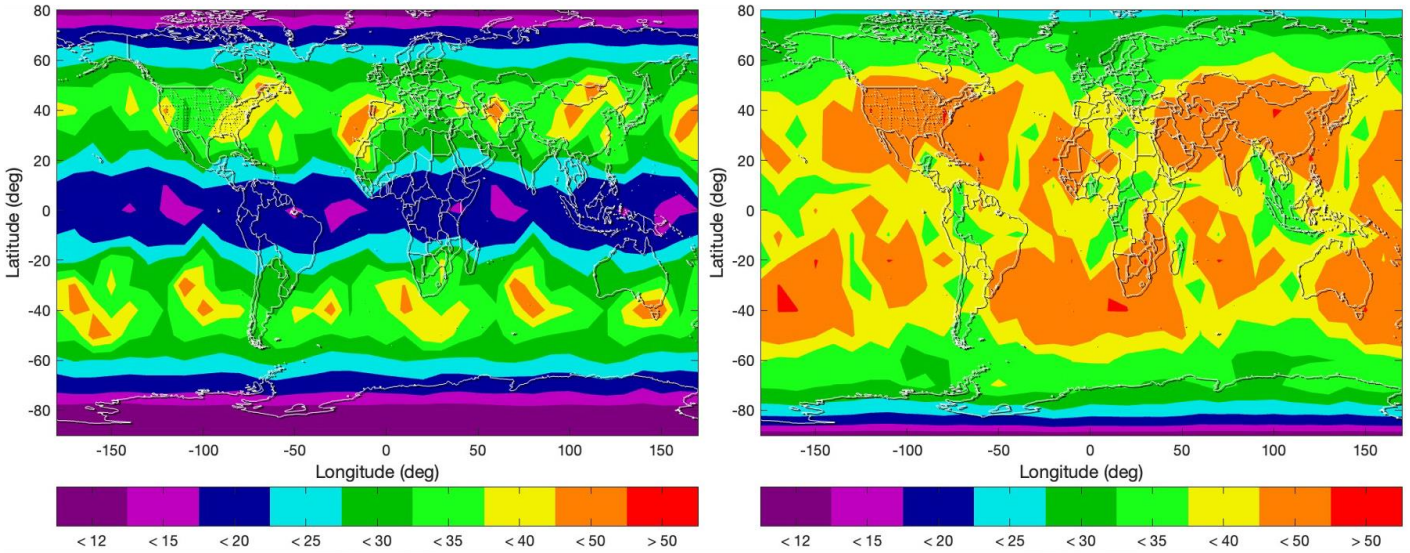

Figure 14: *ARAIM 95th Percentile HPL and VPL for 30-SV GPS and IridiumNext Satellites with 30° Mask Angle*

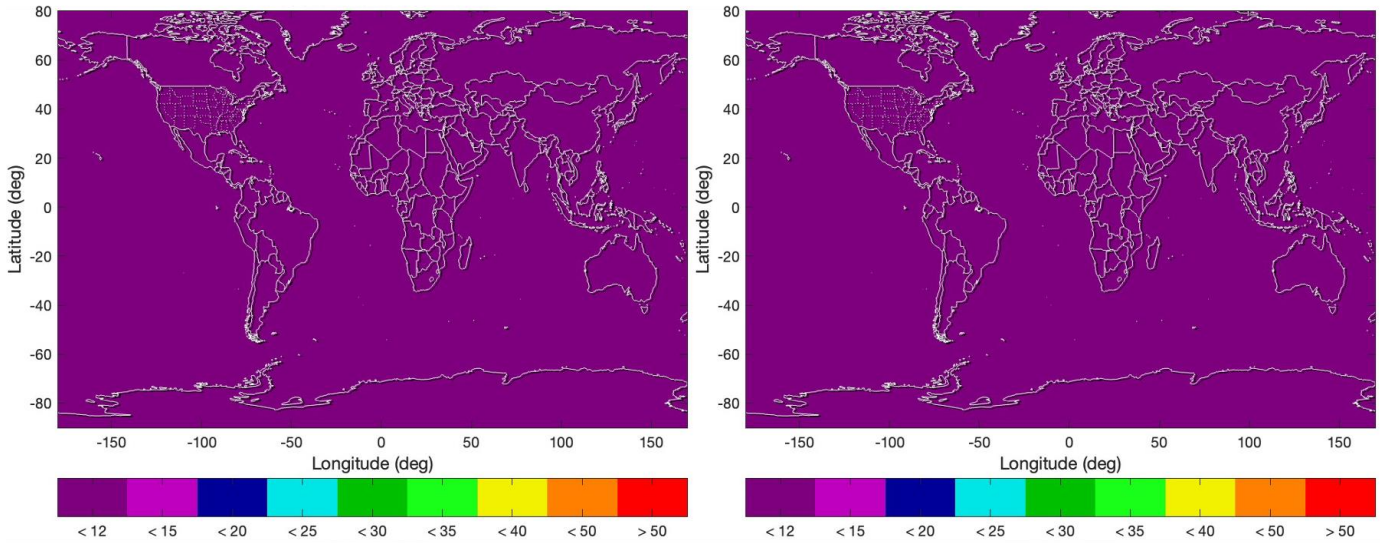

Figure 15: *ARAIM 95th Percentile HPL and VPL for 30-SV GPS and OneWeb Satellites with 5° Mask Angle*

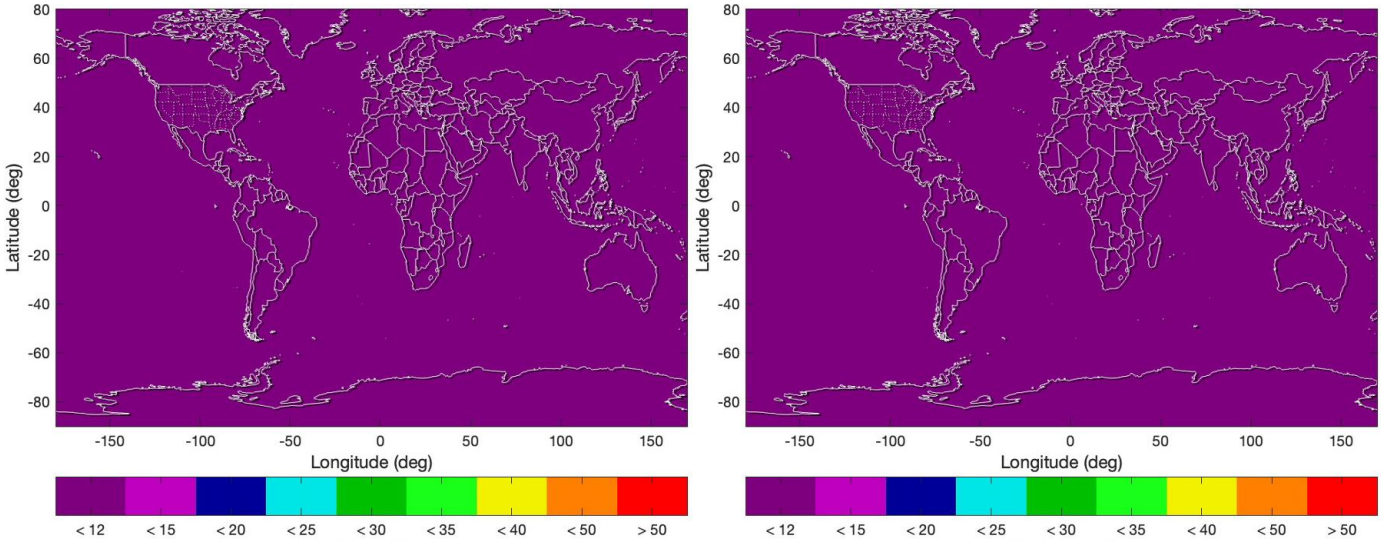

Figure 16: *ARAIM 95th Percentile HPL and VPL for 30-SV GPS and OneWeb Satellites with 15° Mask Angle*

Finally, there are three OneWeb Figures with mask angles of 5°, 15°, and 30°. Figure 16 is the figure shown previously with the baseline mask angle of 5°, while Figures 16 and 17 are the contour plots with mask angles of 15° and 30°, respectively. Note that in all these plots, the zoomed in contour scale is not being used – the original scale used for OneWeb, and the other LEO satellite constellations has been applied here. For OneWeb, increasing the mask angles from 5° to 15° has no visible effect on the HPL and VPL bounds with this contour scale, although some degradation does occur below the 12-meter lower extent of this scale. Further increasing the mask angle from 15° to 30° shows minimal impact on HPL and no impact on VPL for this contour scale. The reason behind why HPL is visibly affected while VPL is unclear and needs further investigation, since VPLs typically have higher bounds than HPLs. Overall, even with a mask angle of 30 degrees, the bounds on both HPL and VPL are exceptional and are likely caused by the sheer number of satellites available in the OneWeb satellite constellation for use in the ARAIM algorithm.

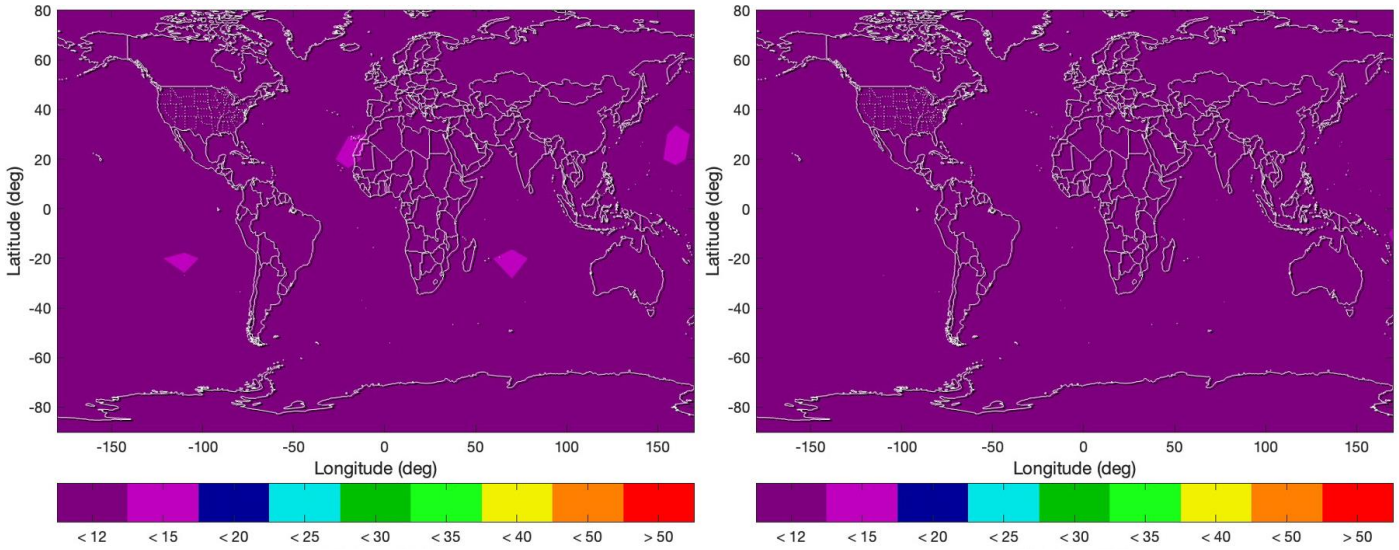

Figure 17: *ARAIM 95th Percentile HPL and VPL for 30-SV GPS and OneWeb Satellites with 30° Mask Angle*

5.2 GPS with LEO Augmentation with Less-Optimistic P_{sat} and Mask Angle Combinations

Figure 18 shows the HPL and VPL contours that were presented as the Globalstar baseline and will be used for comparison against the contours of Figure 19 and 20. While Figure 18 used the baseline assumptions, with a mask angle of 5° and a P_{sat} of 5×10^{-7} from Figure 1, Figure 19 first increases P_{sat}, by one order of magnitude, to 5×10^{-6}. Next, Figure 20 increases the mask angle from 5° to 15° while retaining the higher P_{sat} of 5×10^{-6}.

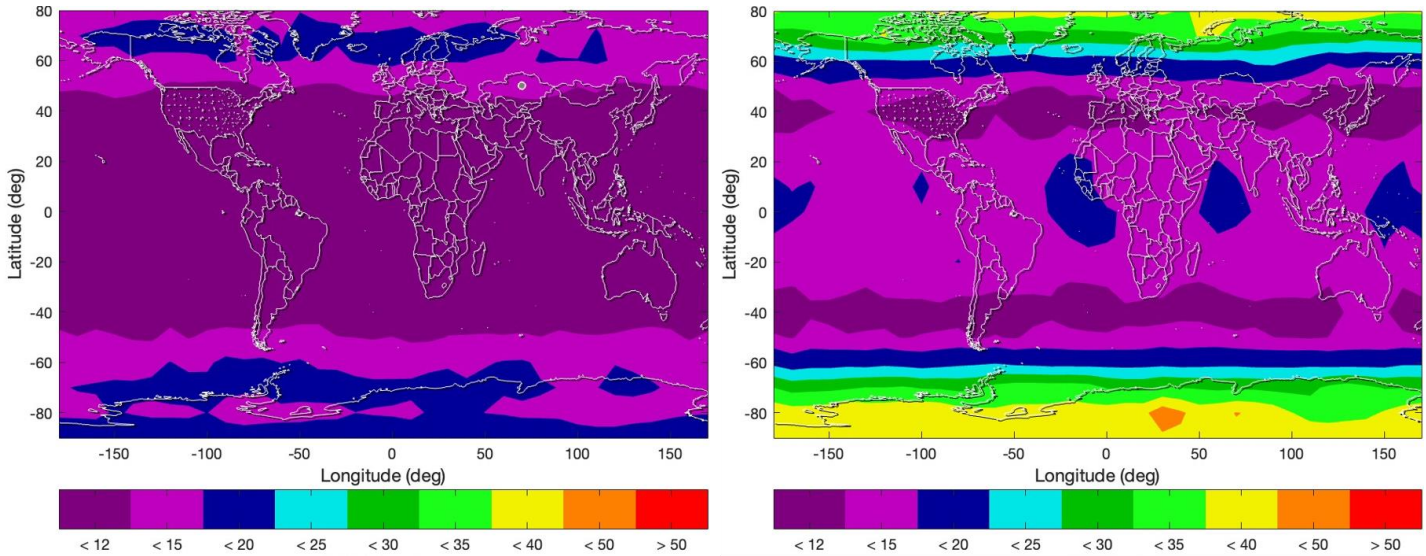

Figure 18: *ARAIM 95th Percentile HPL and VPL for 30-SV GPS and Globalstar Satellites with 5° Mask and $P_{sat} = 5 \times 10^{-7}$*

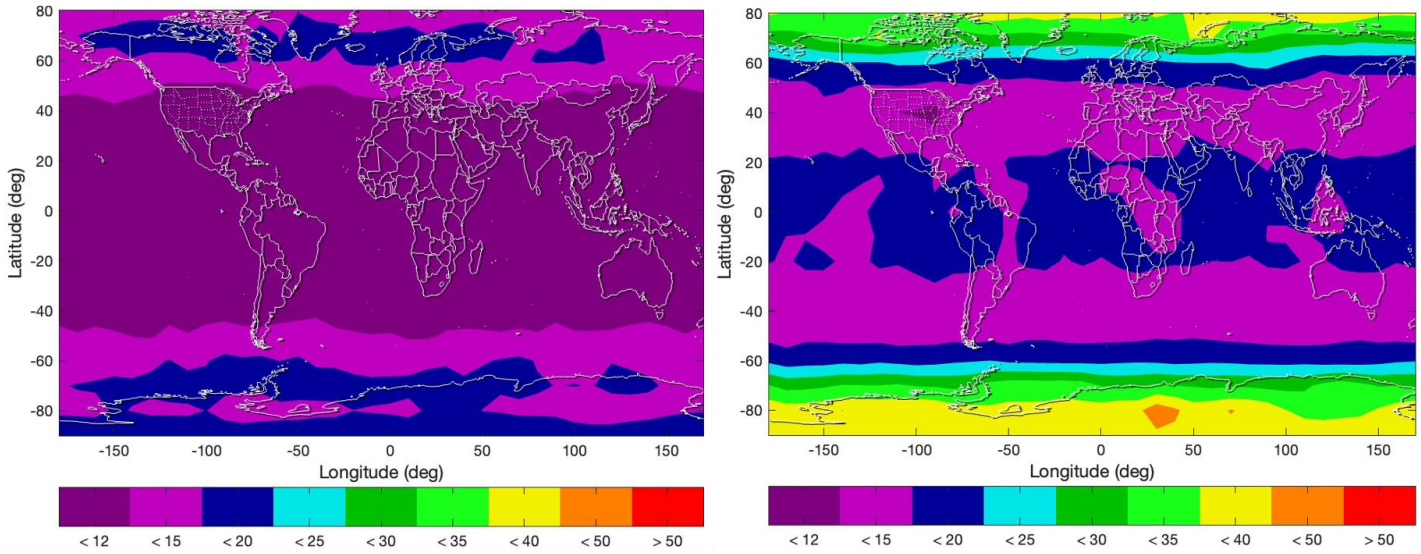

Figure 19: *ARAIM 95th Percentile HPL and VPL for 30-SV GPS and Globalstar Satellites with 5° Mask and* $\boldsymbol{P_{sat} = 5 \times 10^{-6}}$

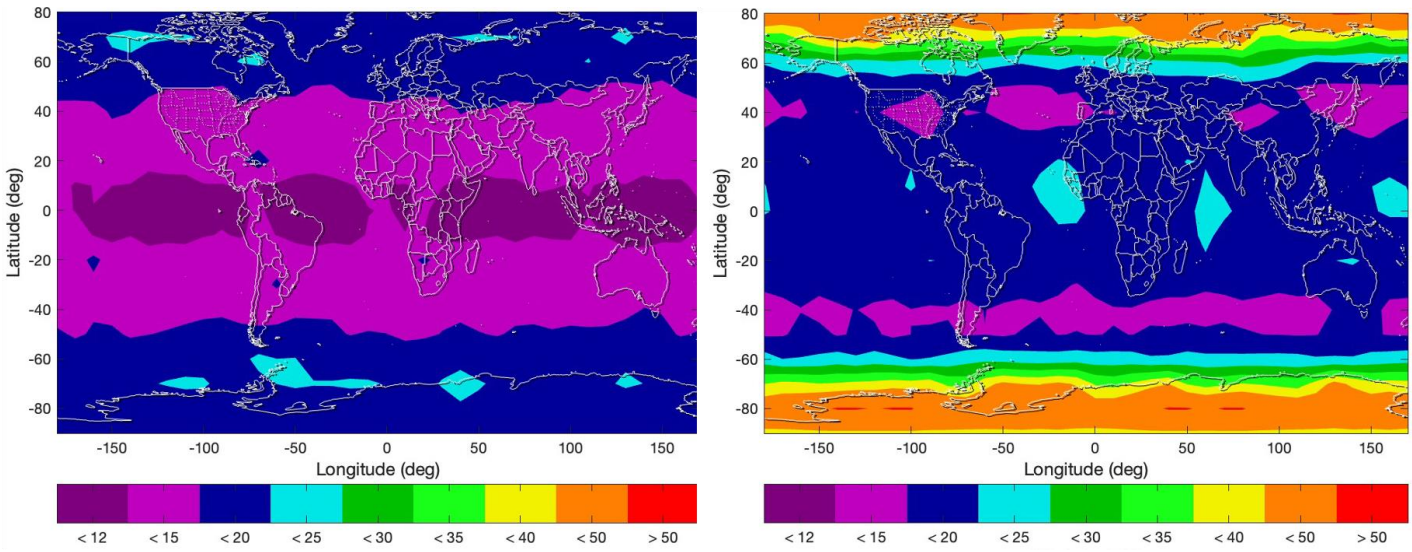

Figure 20: *ARAIM 95th Percentile HPL and VPL for 30-SV GPS and Globalstar Satellites with* ***15° Mask*** *and* $\boldsymbol{P_{sat} = 5 \times 10^{-6}}$

Comparing Figure 19 to Figure 18, the contours for both HPL and VPL are very similar, with the increase in P_{sat} only providing a marginal degradation in the bounds. Because there are only 85 LEO satellites in this constellation, even with this higher P_{sat}, the ARAIM algorithm does not need to consider the probability of two independent satellite fault combinations, which would greatly increase the runtime of the algorithm and further weaken performance. Next, increasing the mask angle to 15° provides similar levels of degradation as the similar cases shown before, with a drop of roughly one to two color bands, representing an increase of 5 to 10 meters in the bounds. However, there remains a clear advantage to using LEO augmentation via Globalstar satellites compared to the results produced by the GPS only simulation. Even with these less idealistic assumptions, around the equator and mid latitudes, 95% HPL is bounded by less than 15 meters, and even at the poles were Globalstar augmentation is the weakest, 95% HPL is bounded by less than 20 meters. For VPL, around the equatorial regions and midlatitudes, the 95% bound is less than 20 meters, although performance degrades rapidly approaching the poles.

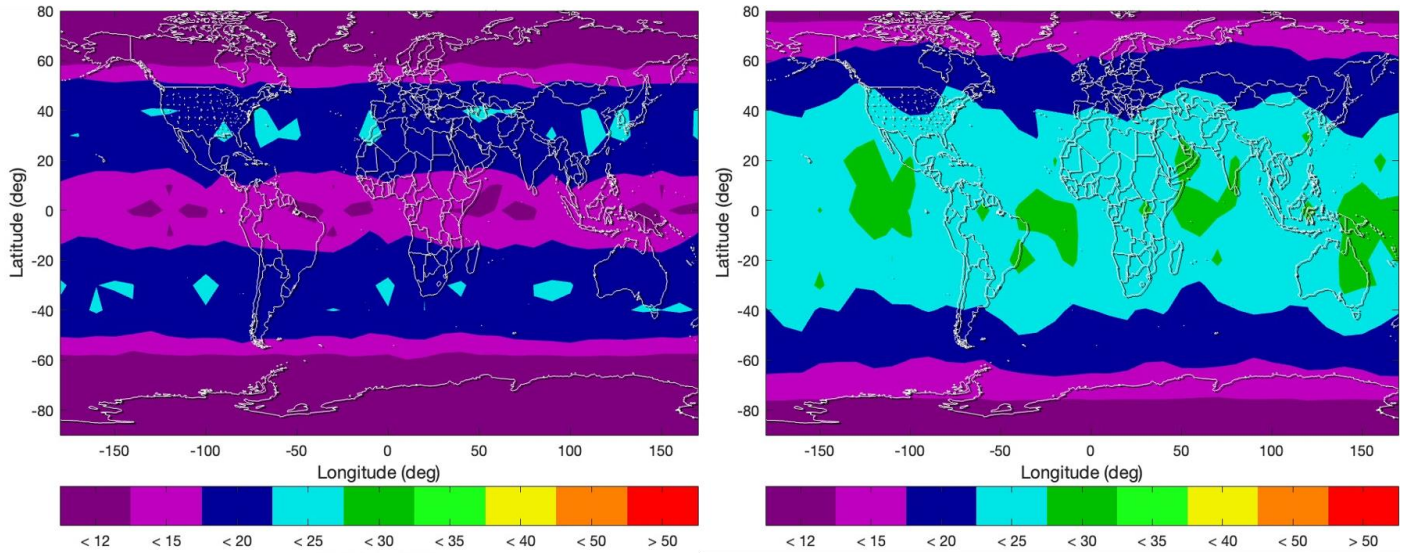

Figure 21: *ARAIM 95th Percentile HPL and VPL for 30-SV GPS and IridiumNext Satellites with 5° Mask and $P_{sat} = 5 \times 10^{-7}$*

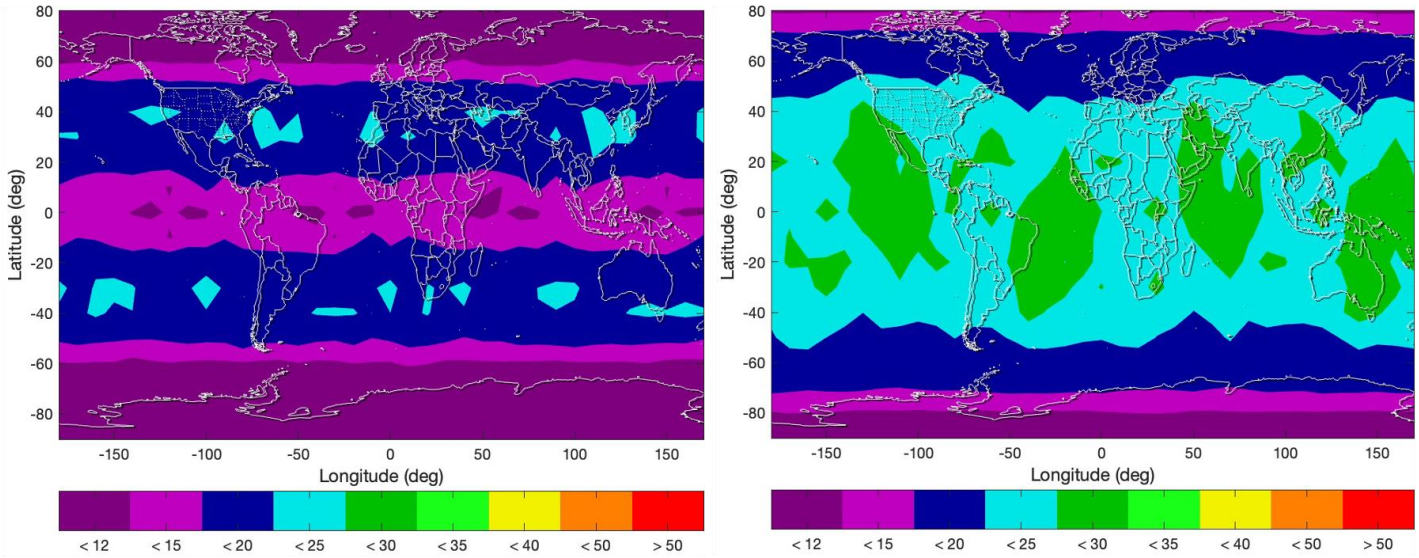

Figure 22: *ARAIM 95th Percentile HPL and VPL for 30-SV GPS and IridiumNext Satellites with 5° Mask and* $\boldsymbol{P_{sat} = 5 \times 10^{-6}}$

Figure 21 shows the HPL and VPL contours that were presented as the baseline results for IridiumNext and are used for comparison against the contours of Figure 22 and 23. While Figure 21 used the idealistic assumptions, with a mask angle of 5° and a P_{sat} of 5×10^{-7}, Figure 22 first increases the P_{sat}, by one order of magnitude, to 5×10^{-6}. Next, Figure 23 increases the mask angle from 5° to 15° while maintaining the higher P_{sat} of 5×10^{-6}. Note that this is the same order of operations that was applied to generate the Globalstar augmented results from Figures 18-20.

The results of changing these parameters for the 75 IridiumNext satelliteshave very similar results to those for Globalstar. Comparing Figure 21 to 22, the contours for both HPL and VPL are very similar, with the increase in P_{sat} only providing a marginal degradation to the 95% PLs. Next, increasing the mask angle to 15° provides similar levels of degradation as the other cases going from 5° to 15°, with a rough drop of one to two color bands, representing an increase of 5 to 10 meters in the bounds. However, just like augmentation using the Globalstar satellites, with these two more realistic assumptions for the LEO satellite parameters, there are clear benefits to LEO augmentation via IridiumNext compared to GPS only. Even with these less idealistic assumptions, around

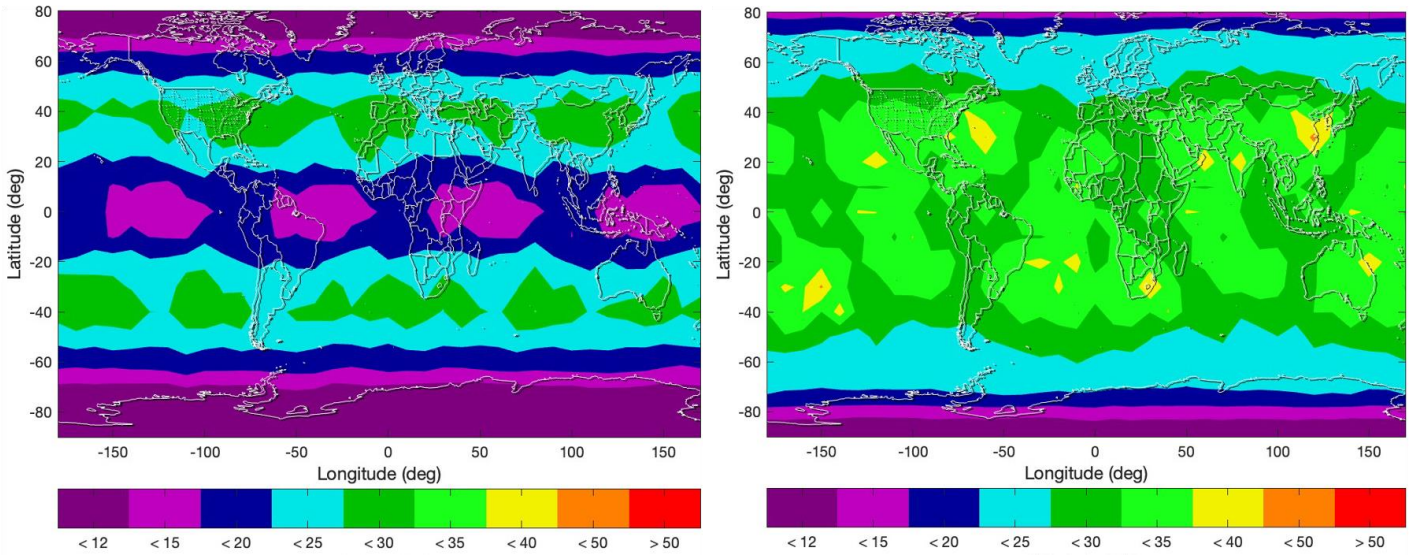

Figure 23: *ARAIM 95th Percentile HPL and VPL for 30-SV GPS and IridiumNext Satellites with* ***15° Mask*** *and* $\boldsymbol{P_{sat} = 5 \times 10^{-6}}$

the poles where IridiumNext performs the best, both 95% HPL and VPL are bounded by less than 12 meters. Even at the equatorial and mid latitude regions, where IridiumNext augmentation is the weakest, 95% HPL is largely bounded by less than 25 meters, and 95% VPL is largely bounded by less than 35 meters.

6. RESULTS FOR LEO-AUGMENTED GPS AT THE 99.9TH PERCENTILE

6.1 GPS with Globalstar Augmentation at the 99.9th Percentile

The previous results have all presented HPL and VPL contour levels at the 95th percentile, which is what an ARAIM user would typically expect. However, for planning purposes it is also important to consider the largest PLs over a given day. This is given by the 99.9th-percentile results, as this percentile results in the largest PLs for each user over the 720 simulated epochs (at 2-minute intervals) over a day. Figure 24 shows the same Globalstar results with a mask angle of 5° from Figure 5 and Figure 9, but at the

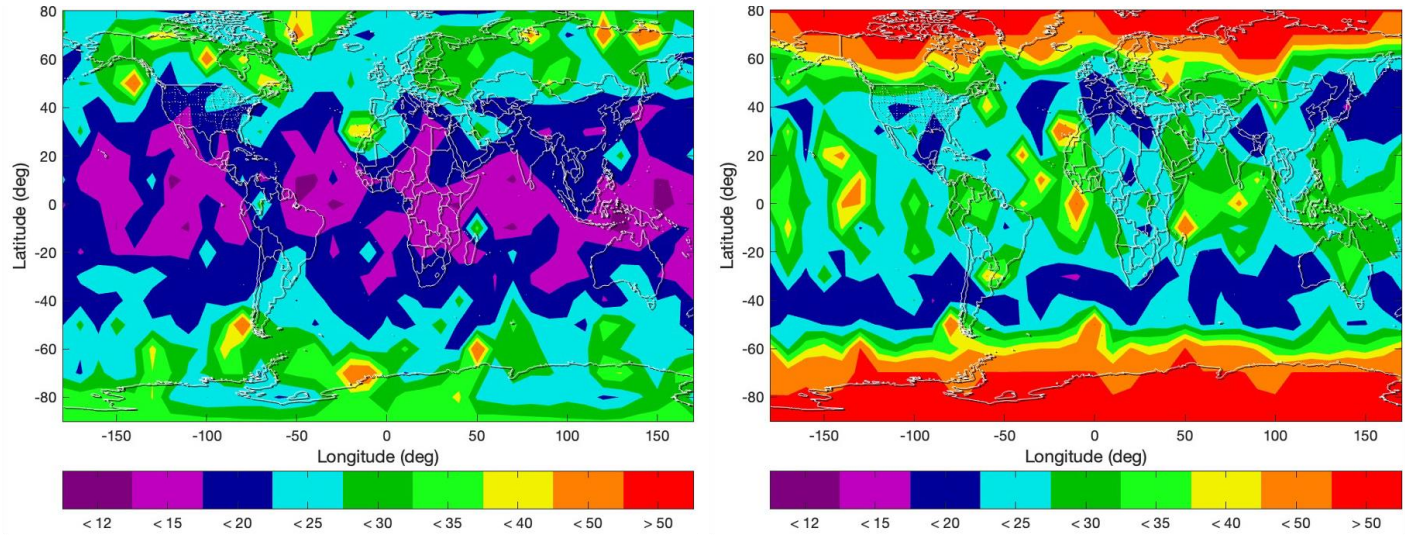

Figure 24: *ARAIM 99.9th Percentile HPL and VPL for 30-SV GPS and 85 Globalstar Satellites with 5° Mask*

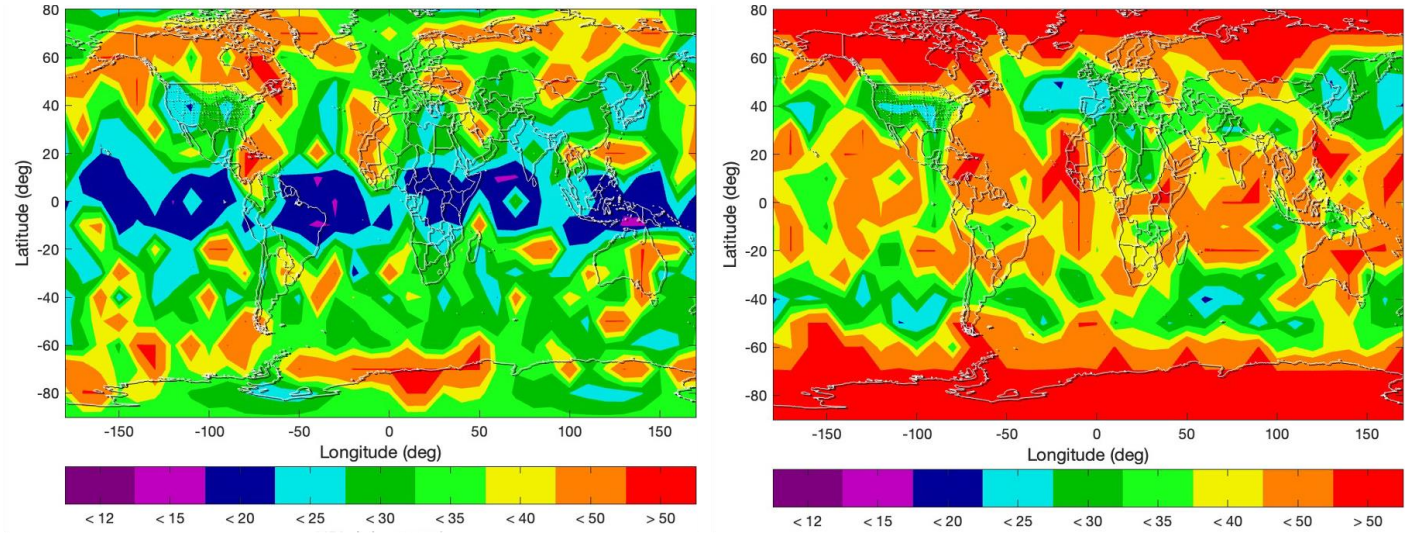

Figure 25: *ARAIM 99.9th Percentile HPL and VPL for 30-SV GPS and 85 Globalstar Satellites with 15° Mask*

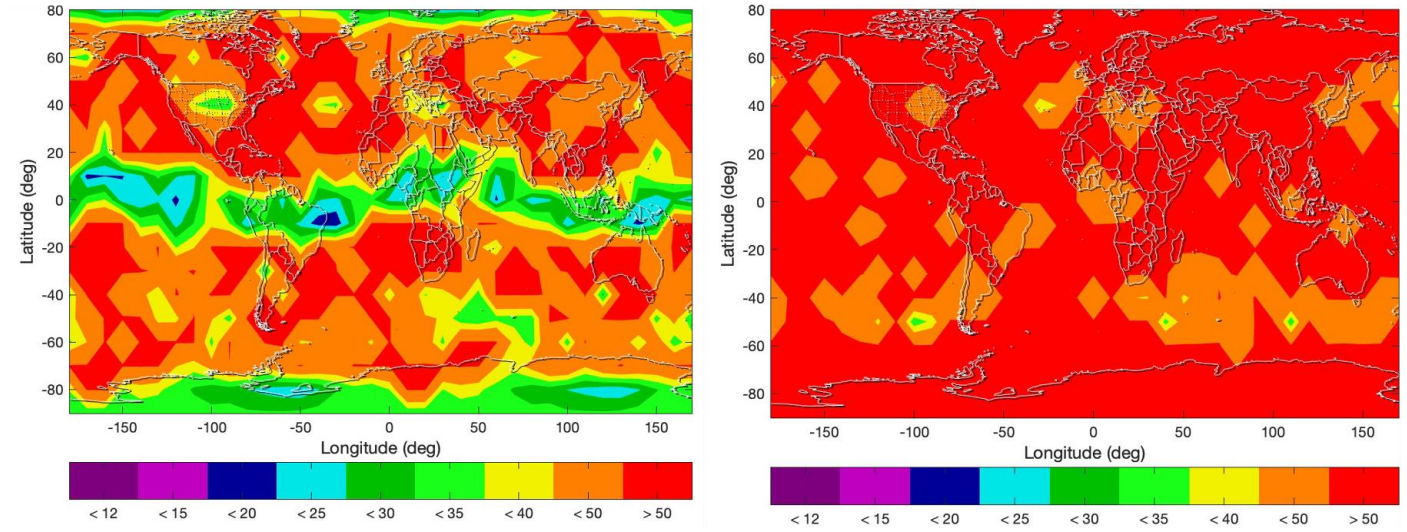

Figure 26: *ARAIM 99.9th Percentile HPL and VPL for 30-SV GPS and 85 Globalstar Satellites with 30° Mask*

99.9th percentile rather than the 95th percentile. Figure 25 shows Globalstar augmented results with a mask angle 15° degrees (Figure 10) at the 99.9th percentile, and Figure 26 shows Globalstar augmented results with a mask angle 30° degrees (Figure 11) at the 99.9th percentile.

As expected, the 99.9th-percentile bounds are significantly larger than the same bounds at the 95th percentile. For example, comparing Figure 24 to the (identical) Figures 5 and 9, a degradation in the PL bounds of about 1 to 3 color bars is typical. Comparing Figures 11 and 26 for a 30° elevation mask angle, the degradation is larger, as most user locations in Figure 26 have 99.9th-percentile PL bounds exceeding 40 meters (orange or red color bands) compared to below 25 meters at the 95th-percentile in Figure 11. The 99.9th-percentile bounds also vary more over shorter distances, which is not surprising because the variation in maximum PLs (which the 99.9th-percentile bounds represent) is expected to be larger than that of PLs below the maximum.

7. SUMMARY AND ONGOING WORK

This paper illustrates the potential for augmenting the GPS constellation with additional ranging satellites in Low Earth Orbits (LEO). Under the idealized assumption that LEO satellites provide the same ranging quality and fault rates as GPS satellites, the improvement in ARAIM protection levels is tremendous because of the benefits of adding so many additional ranging sources to GPS satellite geometries. As these assumptions are made more realistic in terms of LEO satellites having larger elevation mask angles and per-satellite fault probabilities, the benefits weaken somewhat but are still substantial.

Ongoing work on LEO satellite augmentation focuses on two aspects. The first is expanded sensitivity studies that incorporate further increasing the satellite fault probability P_{sat} above 5×10^{-6} and increasing the error variances for LEO satellites well above those for GPS. Further increases in P_{sat} create the likelihood that the probability of two or more simultaneous independent satellite faults is no longer negligible, which would dramatically increase ARAIM processing time and make real-time use infeasible. To counteract this, individual LEO satellites will be grouped into categories based on orbit plane or satellite launch date so that fewer independent fault hypotheses need to be considered (see Blanch (2018a) for more on this approach and Blanch (2018b) for a simpler approach that provides a more conservative bound on PLs). The second is expanding the set of simulated LEO constellations to include the existing Starlink constellation and the purpose-built LEO navigation constellation being developed by Xona Space Systems (Reid, 2021). The many thousands of Starlink satellites will require consideration of multiple simultaneous independent satellite faults. In this case, the conservative approach of Blanch (2018b) is likely to be more practical and may temper somewhat the benefits achieved from having so many visible LEO satellites.

8. REFERENCES

(Ardito, 2019) Ardito, C., Morales, J., et al., "Performance Evaluation of Navigation Using LEO Satellite Signals with Periodically Transmitted Satellite Positions," *Proceedings of ION ITM 2019*, Reston, VA, Jan. 2019, 306-318. https://doi.org/10.33012/2019.16743

(Blanch, 2015) Blanch, J. et al. (2015), "Baseline advanced RAIM user algorithm and possible improvements," *IEEE Transactions on Aerospace and Electronic Systems*, 51(1), 713-732. https://10.1109/TAES.2014.130739

(Blanch, 2018a) Blanch, J. Walter, T., Enge, P. (2018), Fixed Subset Selection to Reduce Advanced RAIM Complexity," *Proceedings of ION ITM 2018*, Reston, VA, Jan. – Feb. 2018, 88-98. http://web.stanford.edu/group/scpnt/gpslab/pubs/papers/Blanch_IONITM_2018_FixedSubsetARAIM.pdf

(Blanch, 2018b) Blanch, J. Blanch, J. Walter, T., Enge, P. (2018), " A Formula for Solution Separation without Subset Solutions for Advanced RAIM," *Proceedings of IEEE/ION PLANS 2018*, Monterey, CA, April 2018, 316-326. http://web.stanford.edu/group/scpnt/gpslab/pubs/papers/Blanch_IEEEIONPLANS_2018_ARAIM.pdf

(Celestrak) Celestrak Orbit Elements (website), https://celestrak.org/NORAD/elements/gp.php?GROUP=globalstar&FORMAT=tle

(ICAO, 2020) "Proposed amendments to Annex 10, Volume I: Global Positioning System (GPS) provisions," ICAO Navigation Systems Panel (NSP), Sixth Meeting, WP 2, November 2020. https://store.icao.int/en/annexes/annex-10

(Katz, 2021) Katz, A., Pullen, S., et al. (2021), "ARAIM for Military Users: ISM Parameters, Constellation-Check Procedure and Performance Estimates," *Proceedings of ION ITM 2021* (Virtual), 173-188. http://web.stanford.edu/group/scpnt/gpslab/pubs/papers/Katz_ION_ITM2021_Military_ARAIM.pdf

(MAAST) "Matlab Algorithm Availability Simulation Tool," Stanford University GPS Laboratory, https://gps.stanford.edu/resources/tools/maast

(Milestone 3, 2016) "Milestone 3 Report of the E.U.-U.S. Cooperation on Satellite Navigation Working Group C: ARAIM Technical Subgroup," Final Version, Feb. 25, 2016. https://www.gps.gov/policy/cooperation/europe/2016/working-group-c/

(Pullen, 2018) Pullen, S., Kilfeather, J., et al., "Enhanced Navigation, Robustness, and Safety Assurance for Autonomous Vehicles as Part of the Globalstar Connected Car Program," *Proceedings of ION GNSS+ 2018*, Miami, FL, Sept. 2018, 1538-1565. https://doi.org/10.33012/2018.16106

(Pullen, 2021) Pullen, S., Lo, S., et al., "Ground Monitoring to Support ARAIM for Military Users: Alternatives for Rapid and Rare Update Rates," *Proceedings of ION GNSS+ 2021*, St. Louis, MO (Virtual), Sept. 2021 (presentation only). http://web.stanford.edu/group/scpnt/gpslab/pubs/papers/Pullen_IONGNSS_2021_Mil_ARAIM.pdf

(Pullen, 2022) Pullen, S., Lo, S., et al., "Inclined Geosynchronous Satellite Augmentation to Maximize Availability of Integrity for Future SBAS and ARAIM Users," *Proceedings of ION ITM 2022*, Long Beach, CA, Jan. 2022 (presentation only). http://web.stanford.edu/group/scpnt/gpslab/pubs/papers/Pullen_ION_ITM_2022_Inclined_GEO_Integrity_Availability.pdf

(Pullen, 2023) Pullen, S., Lo, S., et al., "GNSS Constellation Performance Using ARAIM with Inclined Geosynchronous Satellite and Low-Earth-Orbit Satellite Augmentation," *Proceedings of ION ITM 2023*, Long Beach, CA, Jan. 2023. http://web.stanford.edu/group/scpnt/gpslab/pubs/papers/Pullen_ION_ITM_2023_ARAIM.pdf

(Rabinowitz, 2000) Rabinowitz, M., *A Differential Carrier-Phase Navigation System Combining GPS with Low Earth Orbit Satellites for Rapid Resolution of Integer Cycle Ambiguities*, Ph.D. Dissertation, Stanford University, Dept. of Aeronautics and Astronautics, December 2000. http://web.stanford.edu/group/scpnt/gpslab/pubs/theses/MatthewRabinowitzThesis01.pdf

(Reid, 2021) Reid, T., "Opportunities in Commercial LEO Satellite Navigation," *Proceedings of ION GNSS+ 2021*, St. Louis, MO, Sept. 2021, 2012-2048. https://doi.org/10.33012/2021.18106

(SPS, 2020) *GPS Standard Positioning Service (SPS) Performance Standard (GPS SPS PS)*, Washington DC, U.S. Dept. of Defense, 5th Edition, April 2020. https://www.gps.gov/technical/ps/2020-SPS-performance-standard.pdf